Hybrid state-feedback sliding-mode controller using fuzzy logic for four-wheel-steering vehicles

ALIREZA ALFI[†] MOHAMMAD FARROKHI[†‡]*
[†]Department of Electrical Engineering
[‡]Center of Excellence for Power System Automation and Operation
Iran University of Science and Technology
Narmak, Tehran 16846-13114, Iran
*Corresponding author. Email: farrokhi@iust.ac.ir

This paper presents a fuzzy controller for high-speeds four-wheel-steering vehicles based on the state feedback and the sliding-mode control methods. In the proposed fuzzy controller, the consequent part of the fuzzy *IF-THEN* rules consists of either a sliding-mode controller or a state-feedback controller. Also, it will be proved that, if every fuzzy rule is stable in the sense of Lyapunov for a general Lyapunov function, defined for the whole system, then the whole system is stable in the sense of Lyapunov. The effectiveness of the proposed method for handling improvement of the four-wheel-steering systems will be demonstrated by simulations using a nonlinear vehicle model. The simulation results show that the proposed control method can enhance the dynamic response of the four-wheel steering vehicles by reducing the transient response time and improving vehicle stability as compared to the sliding-mode and the fuzzy sliding-mode control methods.

Keywords: Four-wheel-steering vehicles; Sliding-mode control; State-feedback control; Hybrid fuzzy controller; Stability

1 Introduction

There are three categories for vehicle characteristics: 1) performance, 2) ride and suspension, and 3) handling [1]. The latter characteristic deals with the vehicle response to the driver command controls and inputs, affecting moving directions of the vehicle, as well as stability of the vehicle against environment disturbances. The vehicle and the driver compose a closed-loop system. In other words, the driver acts as a controller and as an actuator. He performs these actions using the steering wheel, the gas and the break pedals, respectively, to achieve a desired movement. Therefore, the steering system directly affects the response of the vehicle [1].

As Fig. 1 shows, when the front and the rear wheels have different slip angles, the vehicle either understeers or oversteers. The understeer condition takes place when the slip angle of the front tyres is greater than the slip angle of the rear tyres. In this situation, a greater steering angle is required to maintain the turning angle. But when the steering angle reaches full lock, the turning angle cannot be maintained and the vehicle drifts to the outside. On the other hand, during oversteering, the slip angle of the rear wheels is greater than the front wheels. Consequently, the turn-rate increases by itself and the driver has to reduce the steering angle to compensate. During severe oversteer, the steering angle may reach full lock in the opposite direction while the vehicle continues on into the turn. A vehicle that understeers is considered safer for average drivers.

The ever-growing demand for better handling of the two-wheel-steering system, which is inspired from the carriage commanding and has been used for several decades, has attracted much attention of the automobile industry to the four-wheel-steering (4WS) systems. In this system, the rear wheels are steered, like the front wheels and in the same direction, in order to improve the manoeuvrability and to increase stability of the vehicle at high speeds.

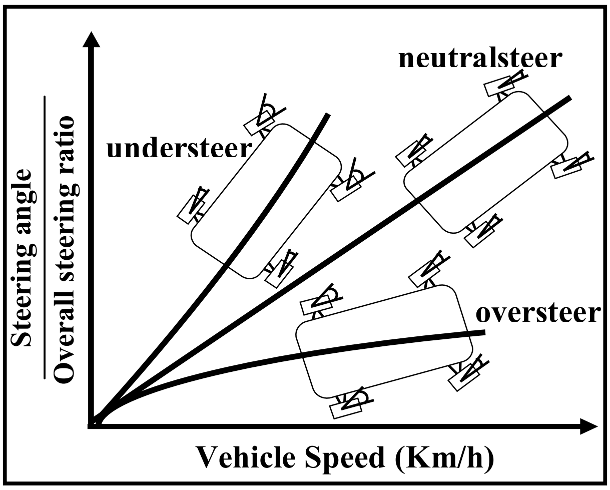

Fig. 1: vehicle handling properties.

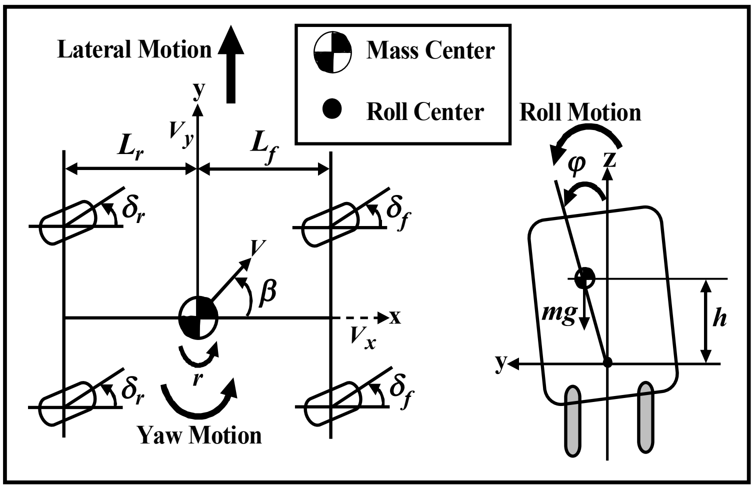

Fig. 2: Three degree of freedom model of 4WS vehicle.

Expressing the above phrases in technical terms, the aim of the 4WS system is to reduce the body side-slip angle at vehicle mass centre. In other words, the phase difference between the yaw rate response and the lateral velocity has to be minimized [2]. This action produces slip angles in rear wheels without the need for the body side-slip angle. Moreover, it eliminates the time delay between the input from the steering and the side force build-up. As a result, the vehicle manoeuvrability substantially increases so that the vehicle's radius of gyration is decreased [3].

Although there are other 4WS systems, which are used for other purposes, such as moving and parking vehicles in very tight places at low speeds, but the focus of this paper is on the 4WS systems in which the rear wheels are steered in the same direction as the front wheels at high speeds.

Several control methods and algorithms, such as proportional control, delay control, phase reversal control, and ideal control, have been proposed for the 4WS systems [4-16]. The control law for steering rear wheels and the model used for the control law are two distinct characteristics for analyzing the 4WS problem. In general, there is controversy among researchers of how the rear wheels should be steered in order to optimize the handling performance and to insure stability of the vehicle. There are two distinctive characteristics which define the approach to this problem: 1) the control law used to steer the rear wheels and 2) the model used to assess the impact of the control law on the dynamics of the vehicle [3], [4]. The latter characteristic is important because the vehicle model is highly nonlinear, which makes it too complicated for use in the controller design procedure. Alfi et al. proposed a new control method for improvement handling of the 4WS systems [17]. The main features of this control method are its simple design procedure and employing the fuzzy logic in 4WS systems.

In recent years, researchers have extensively used the fuzzy logic for modelling, identification and control of highly nonlinear dynamic systems. One drawback of fuzzy systems is the lack of systematic methods to define fuzzy rules and fuzzy membership functions [18]. In addition, the stability analysis of fuzzy controllers is another disputing subject among researchers. Recently, some methods have been proposed in literature to show the stability of closed-loop systems using fuzzy controllers. Among these is the Takagi-Sugeno-Kang (TSK) fuzzy system, in which the stability of each fuzzy subsystem (i.e. each fuzzy rule, which is called the local fuzzy subsystem) can be guaranteed using Lyapunov direct method [19]. The main difficulty using this method is finding a unified Lyapunov function for all subsystems, since usually there are too many fuzzy rules, which is common in fuzzy systems with a few inputs and a handful of membership functions for every input.

In addition to design methods based on the TSK fuzzy models, there are other methods such as partitioning the state space into smaller parts and analyzing the stability of every partition of the closed-loop system. The disadvantages of this method are the long time needed for partitioning due to the large number of partitions for many fuzzy rules and the missing possibility of showing graphically the state space partitions for systems of order above two [20].

In this paper, a fuzzy logic controller, which combines the state-feedback controller (SFC) and the sliding-mode controller (SMC) is proposed. In this method, a fuzzy system decides when to use each one of these controllers or a combination of them. Moreover, the transition between the SFC and the SMC, and vice versa, is continuous. The main contributions of this method are three folds: 1) the fuzzy logic controller takes advantage of both classical controllers (i.e. the good transient response of the SMC and the superior steady-state response of the SFC when the system is working around the operating point). 2) The stability of the closed-loop system is guaranteed when the subsystems (i.e. the SMC and the SFC) are stable. In addition, analyzing the stability is simple since a general Lyapunov function can be defined for the SMC as well as for the SFC. 3) Defining fuzzy rules is effortless. The closed-loop system can work perfectly well with only three rules. Hence, finding a common Lyapunov function for three subsystems (i.e. three fuzzy rules) is not a difficult task. Furthermore, since no fuzzy plant model is involved, the number of subsystems is relatively small, and the common Lyapunov function can be found more easily.

The effectiveness of the proposed method for handling improvement of the 4WS systems will be demonstrated by simulations using a nonlinear model for the vehicles. The simulation results show that the proposed control method can enhance the dynamic response of the 4WS vehicles by reducing the transient response time and improving the vehicle stability as compared to the classical SMC and the fuzzy SMC control methods.

This paper is organized as follows: Section 2 presents the vehicle-handling model, which consists of the vehicle model, the tyre model, and the reference model. The proposed control method will be given in Section 3. The analytical work and the proof of stability for the proposed controller are described in Section 4. Section 5 shows the simulation results, followed by conclusion in Section 6.

2 Vehicle Handling Model

The simplest model used to investigate the vehicle response is the two-degree of freedom bicycle model. This model combines left and right wheels, lumped together at the front and rear of vehicle. Also, the tyre forces are generated at a constant rate proportional to the slip angles. In this paper, a nonlinear three-degree-of-freedom model for the 4WS vehicle has been employed. This model contains the lateral velocity V_y, the yaw rate r, the roll angle φ and the nonlinear equations for tyres.

2.1 Vehicle Model

This section presents the nonlinear vehicle model. Fig. 2 shows the coordinates system of this model. The coordinate system is fixed to the vehicle, the *xy*-plane stays parallel to the road surface, the *x*-axis is oriented to the front, the *y*-axis points to the left, the *z*-axis is vertically pointing upwards and the origin is located at the roll centre of the vehicle. In Fig. 2, δ_f and δ_r are inputs to the front and the rear steering wheels, respectively. The equations of motion are as follows [21]:

$$m(\dot{V}_y + r V_x) + m_s h\ddot{\varphi} = F_{Yfl} + F_{Yrl} + F_{Yfr} + F_{Yrr} + 2\frac{\partial F_f}{\partial \varphi'_f}\frac{\partial \varphi'_f}{\partial \varphi}\varphi + 2\frac{\partial F_r}{\partial \varphi'_r}\frac{\partial \varphi'_r}{\partial \varphi}\varphi , \tag{1}$$

$$I_{zz}\dot{r} - I_{zx}\ddot{\varphi} = L_f\left[F_{yfl} + F_{yfr} + 2\frac{\partial F_f}{\partial \varphi'_f}\frac{\partial \varphi'_f}{\partial \varphi}\varphi\right] - L_r\left[F_{yrr} + F_{yrl} + 2\frac{\partial F_r}{\partial \varphi'_r}\frac{\partial \varphi'_r}{\partial \varphi}\varphi\right], \tag{2}$$

$$I_{xx}\ddot{\varphi} - I_{xz}\dot{r} + m_s h(\dot{V}_y + r V_x) = -(L_{\varphi f} + L_{\varphi r})\varphi - (L_{\dot{\varphi} f} + L_{\dot{\varphi} r})\dot{\varphi} , \tag{3}$$

where V_x and V_y are the longitudinal and lateral velocities, respectively, r is the yaw rate, φ is the roll angle, m is the total mass of vehicle, m_s is the sprung mass of vehicle, h is the height of the centre of gravity of the sprung mass, L_f and L_r are distances from the front and rear axles to the centre of gravity of vehicle, respectively, $L_{\varphi f}$ and $L_{\varphi r}$ are the roll stiffness produced by the front and rear springs, respectively,

$L_{\dot{\varphi}f}$ and $L_{\dot{\varphi}r}$ are the roll damping produced by the front and rear shock absorbers, respectively, and F_y is the respective tyre lateral force. Indices $fl, fr, rl,$ and rr are designated for the lateral tyre forces corresponding to the front-left, front-right, rear-left and rear-right, respectively. In addition, $\partial F_f / \partial \varphi_f'$ and $\partial F_r / \partial \varphi_r'$ are the change in side force of the front and rear tyres corresponding to the changes in the front and rear camber angle, respectively, $\partial \varphi_f' / \partial \varphi$ and $\partial \varphi_r' / \partial \varphi$ are the change in the front and rear camber angle corresponding to the changes in the roll angle, respectively. Finally, I_{xx}, I_{zz} and I_{xz} are the moments of inertia about the roll axis, the yaw axis and the roll-yaw axis, respectively.

2.2 Tyre Model

Because of the interactions between the tyres and road, the main contribution to the nonlinearity of the vehicle dynamics in different steering maneuvers comes from tyres. Therefore, the stiffness coefficient of tyres plays an important role in the process of vehicle handling. In this case, due to simultaneous occurrence of the lateral and longitudinal slip, mutual influence of the longitudinal and lateral tyre forces is significant. The actual tyre forces depend on the material and geometric parameters of the tyres, the vertical forces, the speed of the vehicle and the road conditions. Therefore, the dynamic behavior of tyres is very complex. Many researchers have tried to define suitable tyre models. In this paper, the following equation is adopted for tyre side forces [21]:

$$F_{yi} = f\,(\alpha_i, N_i), \tag{4}$$

where $i = fl, fr, rl, rr$ denotes the lateral tyre forces corresponding to the front-left, front-right, rear-left and rear-right, respectively, F_{yi}, α_i and N_i are the side force generated by the ith tyre, the slip angle of the ith tyre, and the normal force on the ith tyre, respectively. The tyre side forces are described in Appendix A.

2.3 Reference Model

The desired handling performance of the vehicle can be expressed in terms of a reference model, which gives the desired response of the vehicle to a command signal. A vehicle, which exhibits shorter rise time for the yaw motion and shorter settling time for the directional stability, can be regarded as a good reference model. Moreover, this reference model should have almost zero body side-slip angles at low speeds. Based on these, a desirable yaw reference model should have a suitable damping without oscillations or overshoots. Hence, a first order system can be a good choice for the reference model [23]:

$$\dot{r}_m = -\frac{1}{T_m} r_m + \frac{g(V_x)}{T_m}\delta_f, \tag{5}$$

$$g(v_x) = \frac{V_x}{1 + K_{\text{us}} V_x^2 / g}, \tag{6}$$

$$K_{\text{us}} = \frac{w_f}{c_f} - \frac{w_r}{c_r}, \tag{7}$$

where T_m is the time constant of the reference model, δ_f is the angle of the front wheels, $g(V_x)$ is the steady-state yaw rate gain, which is a function of the vehicle speed V_x, K_{us} is the understeer coefficient, w_f and w_r are the normal static loads at the front and rear axels, respectively, c_f and c_r are the front and rear tyre cornering stiffness coefficients, respectively, and g is the acceleration of gravity. If $K_{\text{us}} > 0$, vehicle is in understeering situation, while $K_{\text{us}} < 0$ defines an oversteered vehicle. As a result, according to [1] the desired vehicle response can be described as

$$V_{y\,\text{des}} = 0, \quad r_{\text{des}} = \frac{V_x}{L + K_{\text{us}} V_x^2}\,\delta_f, \tag{8}$$

where r_{des} and $V_{y\,\text{des}}$ are referred to as the desired yaw rate and the desired lateral velocity of the vehicle, respectively.

3. 4WS Controller Design

This section presents the proposed control method for the 4WS system. In order to design a control system, it is necessary first to establish the targets. The following response characteristics can be considered as the desirable control objectives for the steering system:

1. The steering response can be improved by eliminating resonance peaks in the yaw rate.
2. The orientation of vehicle must align with the actual direction of forward movement (i.e. the side-slip angle at the vehicle's center of gravity should be zero).
3. Better stability against disturbances (i.e. robustness of the controller) is required.
4. The desired steering response characteristics against changes in the vehicle parameters should be maintained.

The equations representing the vehicle and the tyre model are highly nonlinear and the control parameters are highly coupled. Based on this, a controller is proposed that combines the state-feedback control method with the sliding-mode controller using the fuzzy logic. Theses controllers are designed independently in order to provide good performance.

In the followings, a Sliding-Mode Controller (SMC) and a State-Feedback Controller (SFC) for the 4WS system is designed independently. Then, by designing a fuzzy system, these controllers will be blended together in such a way that when the states of the system are far away from the desired values, the SMC defines the inputs to the system. On the other hand, when the states of the system are near the desired values, the SFC is employed. The transition between the SMC and the SFC is continuous and smooth.

3.1 Sliding-Mode Controller Design

The concept of SMC is to choose a suitable surface in the state space, called the sliding surface, and switch the control input on this surface. The SMC input guarantees all trajectories move towards the sliding surface. The SMC is not a model-based controller; it is considered a robust control method and is insensitive to parameter fluctuations and disturbances [24].

In order to improve stability of the 4WS system against disturbances (e.g. the effects of side winds on the vehicle) a SMC is designed, which is robust against disturbances and uncertainties in the vehicle parameters such as e.g. unmodeled non-linear suspension conditions.

The system dynamics are described by the following set of state-space equations:

$$\dot{\mathbf{x}} = \mathbf{f}(\mathbf{x}) + \mathbf{b}(\mathbf{x})\,u\,, \tag{9}$$

where $\mathbf{x} \in \Re^n$ is the state vector, $\mathbf{f}(\mathbf{x})$ and $\mathbf{b}(\mathbf{x})$ are vectors of nonlinear functions and u is the scalar control input. The sliding surface is defined as

$$s(\mathbf{x},t) = \mathbf{c}\,\mathbf{e}\,, \tag{10}$$

where $\mathbf{c} \in \Re^{1\times n}$ is a positive vector and $\mathbf{e} = \mathbf{x} - \mathbf{x}_d \in \Re^{n\times 1}$ is the tracking error between the actual system and the reference model. The sliding surface for the 4WS system can be interpreted as the surface of lateral velocity error and yaw rate error between the system and the reference model.

As s approaches zero, the 4WS tracks the reference model with good accuracy. It will be shown, in section 4, that the control law

$$u_{\text{SMC}} = \hat{u} - \left(\mathbf{c}\,\mathbf{b}(\mathbf{x})\right)^{-1} k_d \operatorname{sgn}(s)\,, \tag{11}$$

where $\hat{u} = -\left(\mathbf{c}\,\mathbf{b}(\mathbf{x})\right)^{-1} \mathbf{c}\,\mathbf{f}(\mathbf{x})$ and k_d is a positive constant (called the switching gain), can satisfy the sliding condition

$$\frac{1}{2}\frac{d}{dt}s^2 \le \eta\,|s|\,, \tag{12}$$

with the sign function defined as

$$\text{sgn}(s)=\begin{cases}1 & \text{if } s>0\\ 0 & \text{if } s=0\\ -1 & \text{if } s<0.\end{cases} \tag{13}$$

This controller shows high frequency switching (called the chattering phenomena) near the sliding surface due to the sign function involved. The chattering may excite the vehicle body structure which can lead to severe shaking e.g. of the steering system. The chattering phenomena can be avoided by introducing a boundary layer with the width of ε around the sliding surface. Replacing $\text{sgn}(s)$ in (11) with $\text{sat}(s/\varepsilon)$, gives

$$u_{\text{SMC}}=\hat{u}-\left(\mathbf{c}\mathbf{b}(\mathbf{x})\right)^{-1}k_d\,\text{sat}\left(\frac{s}{\varepsilon}\right), \tag{14}$$

where

$$\text{sat}(\mathbf{x})=\begin{cases}\text{sgn}(\mathbf{x}) & \text{when } |\mathbf{x}|>1\\ \mathbf{x} & \text{when } |\mathbf{x}|\le 1.\end{cases} \tag{15}$$

3.2 State-Feedback Controller Design

In this section, the 4WS control system will be designed based on a linear model with 2 degrees of freedom. Assuming that the vehicle is working around the operating point (i.e. there is neither roll steer effect nor lateral weight transfer) the state equations of motion can be expressed as follows [25]:

$$\begin{bmatrix}\dot{V}_y\\ \dot{r}\end{bmatrix}=\begin{bmatrix}-2\dfrac{c_f+c_r}{m\,V_x} & -2\dfrac{L_f\,c_f-L_rc_r}{m\,V_x}\\ -2\dfrac{L_f\,c_f+L_rc_r}{I_{zz}\,V_x} & -2\dfrac{L_f^2\,c_f+L_r^2c_r}{I_{zz}\,V_x}\end{bmatrix}\begin{bmatrix}V_y\\ r\end{bmatrix}+\begin{bmatrix}2\dfrac{c_f}{m}\\ 2\dfrac{L_f\,c_f}{I_{zz}}\end{bmatrix}\delta_f+\begin{bmatrix}2\dfrac{c_r}{m}\\ -2\dfrac{L_r\,c_r}{I_{zz}}\end{bmatrix}\delta_r, \tag{16}$$

where c_f and c_r are the front and rear tyre cornering stiffness coefficients, respectively. Other parameters are the same as defined before. Equation (16) can be shown in vector-matrix notation form as

$$\dot{\mathbf{x}}=\mathbf{A}\mathbf{x}+\mathbf{B}_f\,\delta_f+\mathbf{B}_r\delta_r, \tag{17}$$

where

$$\mathbf{A}=\begin{bmatrix}-2\dfrac{c_f+c_r}{m\,V_x} & -2\dfrac{L_f\,c_f-L_r\,c_r}{m\,V_x}\\ -2\dfrac{L_f\,c_f+L_rc_r}{I_{zz}\,V_x} & -2\dfrac{L_f^2\,c_f+L_r^2c_r}{I_{zz}\,V_x}\end{bmatrix},\quad \mathbf{B}_f=\begin{bmatrix}2\dfrac{c_f}{m}\\ 2\dfrac{L_f\,c_f}{I_{zz}}\end{bmatrix},\quad \mathbf{B}_r=\begin{bmatrix}2\dfrac{c_r}{m}\\ -2\dfrac{L_r\,c_r}{I_{zz}}\end{bmatrix}.$$

Reminding the goal of the 4WS system, which is the better handling of the vehicle using additional rear wheel steering, the 4WS control system will be designed using the optimal control theory. Employing Linear Quadratic Regulator (LQR) method, it is desired to minimize the lateral velocity angle of the vehicle using the 4WS. In the design procedure for the SFC, it is assumed that the input to the front wheels is constant (i.e. $\delta_f=\text{const.}$; in other words, the vehicle is around the operating point), which results in minimization of the following performance index:

$$J=\int_0^{\infty}\left(\mathbf{x}^T\mathbf{Q}\,\mathbf{x}+R\,\delta_r^2\right)dt\ , \tag{18}$$

with the following state space equation

$$\dot{\mathbf{x}}=\mathbf{A}\mathbf{x}+\mathbf{B}_f\,\delta_f+\mathbf{B}_r\delta_r, \tag{19}$$

where $R\in\Re>0$ is a weighting parameter and $\mathbf{Q}\in\Re^{n\times n}$ is a positive weighting matrix. The closed-loop response δ_r can be found as [26]

$$\delta_r = -\frac{1}{R}\mathbf{B}_r^T\,\mathbf{P}\,\mathbf{x}\,, \tag{20}$$

where $\mathbf{P}$ is a symmetric positive matrix that satisfies the following algebraic Riccati equation:

$$-\mathbf{PA} - \mathbf{A}^T\mathbf{P} + \mathbf{PB}_r\mathbf{R}^{-1}\mathbf{B}_r^T\mathbf{P} - \mathbf{Q} = 0\,. \tag{21}$$

Therefore, the SFC for rear wheels is

$$u_{\mathrm{SFC}} = -\mathbf{k}^T\mathbf{x}\,, \tag{22}$$

where

$$\mathbf{k} = -\frac{1}{R}\mathbf{B}_r^T\mathbf{P}\,. \tag{23}$$

In the following section, a combination of the SFC and the SMC is developed based on the fuzzy logic.

3.3 Hybrid Controller Design

A combination of the SFC and the SMC is presented in this section. That is, a fuzzy system defines which controller should be used based on the situation of the states in the 4WS system. The transition between the SMC and the SFC is continuous, so there won't be abrupt changes in the input applied to the system. Moreover, the stability of the whole system can be guaranteed, provided that sub-controllers (i.e. the SMC and the SFC) are independently stable. The stability analysis of the proposed controller will be given in Section 4. The fuzzy IF-THEN rules are defined as follows:

$$\begin{aligned}
&\text{Rule1: IF } s \text{ is } P \text{ THEN } u = \hat{u} + (\mathbf{Cb}(\mathbf{x}))^{-1}k_d\,\mathrm{sat}\left(\frac{s}{\varepsilon}\right)\\
&\text{Rule2: IF } s \text{ is } Z \text{ THEN } u = -\mathbf{k}^T\,\mathbf{x}\\
&\text{Rule3: IF } s \text{ is } N \text{ THEN } u = \hat{u} - (\mathbf{Cb}(\mathbf{x}))^{-1}k_d\,\mathrm{sat}\left(\frac{s}{\varepsilon}\right)
\end{aligned} \tag{24}$$

where s (the sliding surface) has been defined as a fuzzy variable in these fuzzy rules. The membership functions for the fuzzy sets P, Z and N are shown in Fig. 3. By using the weighted sum defuzzification method, the crisp output $u_c(\mathbf{x})$ can be obtained as [20]

$$u_c(\mathbf{x}) = \frac{\sum_{\mathrm{i=1}}^{3}\mu_i(\mathbf{x})\,u_i(\mathbf{x})}{\sum_{\mathrm{i=1}}^{3}\mu_i(\mathbf{x})}\,. \tag{25}$$

According to this fuzzy system, when the states of the system are far from the desired states (i.e. far from the sliding surface) then the SMC defines the main control law. In other words, in this case the first and the third rules of (24) are used, respectively. This is due to the fact that the SMC has a very fast transient response and drives the state variables of the system very quickly to the desired states. On the other hand, when the state of the system is close to the desired state, the SFC is employed. I.e. the second rule of (24) is used because a steady-state error of zero virtually can be achieved by the SFC. The transition between the SMC and the SFC is continuous based on (25) and in this case piecewise linear as shown in Fig. 3.

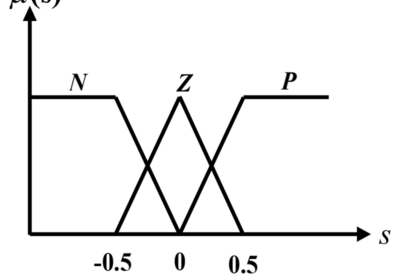

Fig. 3: Membership functions for the switching surface. *N*=Negative, *Z*= Zero, *P*= Positive.

4. Stability Analysis

The idea of stability analysis in this paper is to break down the problem into three fuzzy subsystems, one for every fuzzy rule. The complexity of the analysis is drastically decreased when every subsystem is checked individually. However, the condition that every fuzzy subsystem yields a stable closed-loop system does not directly imply that the whole fuzzy control system, composed of several subsystems, yields a stable closed-loop system. Sufficient conditions that make this implication valid are stated in the following theorem [27], [28].

Theorem: Consider a combined fuzzy logic control system as given in (24) and (25). If

1) there exits a positive-definite, continuously differentiable, and radially unbounded scalar function $V = \mathbf{x}^T \mathbf{P} \mathbf{x}$ where $\mathbf{P} \in \Re^{n \times n}$ is a constant and positive-definite matrix, and
2) every fuzzy subsystem gives a negative-definite $\dot{V}$ in the active region of the corresponding fuzzy rule, and
3) the weighted-sum defuzzification method is employed, which for any input, the output u_c of the fuzzy logic controller lies between u_p and u_q such that $u_p \le u_c \le u_q$, where u_p and u_q are the lower and upper bound of u_c, respectively,

then according to the Lyapunov theory, the equilibrium point at the origin is globally asymptotically stable.

Therefore, to guarantee the system stability, we need to find a suitable Lyapunov function V and ensure that every fuzzy subsystem gives a negative-definite $\dot{V}$ in the active region of the corresponding fuzzy rule. The active region of the corresponding fuzzy rule is defined as region $\mathbf{X}_r \subset \mathbf{X}$, such that the membership function $\mu_i(\mathbf{x_0})$ is not zero for all $\mathbf{x_0} \in \mathbf{X}_r$.

Proof: Consider the Lyapunov function $V = \frac{1}{2} s^2$, where s is the sliding surface, defined in (10) as

$$s = \mathbf{c}\mathbf{e} = \mathbf{c}(\mathbf{x} - \mathbf{x}_d).$$

From the Lyapunov stability theory, it is known that if $\dot{V}$ is negative definite, the system trajectory will be driven towards the sliding surface and remains on it until the origin is reached asymptotically.
The SMC subsystem results in a new sliding control law as

$$u_{\text{SMC}} = \hat{u} - (\mathbf{c}\mathbf{b}(\mathbf{x}))^{-1} k_d \operatorname{sgn}(s).$$

Therefore, it is straightforward to see that

$$\dot{V} = s\dot{s} = s\left[\mathbf{c}\mathbf{f}(\mathbf{x}) + \mathbf{c}\mathbf{b}(\mathbf{x})(-(\mathbf{c}\mathbf{b}(\mathbf{x}))^{-1}(\mathbf{c}\mathbf{f}(\mathbf{x}) + k_d \operatorname{sgn}(s))) \right] = -s\, k_d \operatorname{sgn}(s) = -k_d\,|s| \le 0. \tag{26}$$

Hence, stability of the SMC subsystem is guaranteed.

For the SFC Subsystem, by using the same Lyapunov function $V = \frac{1}{2} s^2$, assuming the linear system

$$\dot{\mathbf{x}} = \mathbf{A}\,\mathbf{x} + \mathbf{B}_r u, \tag{27}$$

and the proposed control law (22), the dynamic equation of the error, by choosing $\mathbf{e} = \mathbf{x} - \mathbf{x}_d$, will be

$$\dot{\mathbf{e}} = \mathbf{A}\mathbf{e} + \mathbf{B}_r u + \mathbf{A}\mathbf{x}_d. \tag{28}$$

It can be shown that if $\mathbf{A}\mathbf{x}_d = 0$, and if the state variables of the new system in (28) converge to zero, then the state variables of the system will converge to $\mathbf{x}_d$. It can be shown that the following state-feedback control law can drive the states of (28) to zero [27]:

$$u_{\text{sfc}} = \left(-\frac{1}{R} \mathbf{B}_r^T \mathbf{P} \right) \mathbf{e}. \tag{29}$$

Hence,

$$\dot{V} = s\,\dot{s} = \mathbf{e}^T\mathbf{c}^T\mathbf{c}\dot{\mathbf{e}} = \mathbf{e}^T\mathbf{c}^T\mathbf{c}\left[\mathbf{A}\mathbf{e} + \mathbf{B}_r\left(-\frac{1}{R}\mathbf{B}_r^T\mathbf{P}\right)\mathbf{e}\right] = \mathbf{e}^T\left\{\mathbf{c}^T\mathbf{c}\left[\mathbf{A} - \mathbf{B}_r R^{-1}\mathbf{B}_r^T\mathbf{P}\right]\right\}\mathbf{e}$$
$$= -\mathbf{e}^T\mathbf{F}\mathbf{e}, \tag{30}$$

where **F** is a positive-definite matrix. Therefore, the state-feedback subsystem is also stable. ∎

5. Simulations

To assess the performance of the proposed controller, the simulations are performed in two parts. First, assuming the vehicle runs on a dry road, the performance of the proposed controller is compared to the SMC, the fuzzy SMC and the 2WS system. In the second part, the proposed controller has been tested against different disturbances, such as cross winds, changes in the road conditions, and variations in the vehicle parameters, i.e. mass, yaw moment of inertia and longitudinal velocity of the vehicle. Moreover, the performance of the proposed controller is compared to the classical SMC and the fuzzy SMC.

In simulations, the yaw rate, the body side-slip angle, the roll angle, and the roll rate will be considered. The input to the front wheels is a step function with amplitude of 0.0345 rad. The vehicle parameters are shown in Table 1. In simulations, a comprehensive tyre model of radial tyre 155R13, with standard cross section radial (RWD), it is used (see Appendix A).

The control law of the SMC is given in (13) and the fuzzy SMC is described in Appendix B.

Recall that the following aims are considered for the 4WS control system:

1- The body side-slip angle goes to zero.

2- Because of good yaw response, the vehicle more accurately follows the desired path during turns without oscillations and with suitable damping.

3- The vehicle moves more rapidly and less smoothly since roll rate is faster.

4- Stability against disturbances (e.g. gusting cross wind) is improved. The vehicle is also more stable at the end of a lane change.

The simulation results are summarized in Figs. 4-10. The results of the first part are shown in Fig. 4. As this Fig. shows, the proposed controller performs better than other controllers. The body side-slip angle is reduced as compared to the SMC, the fuzzy SMC and the 2WS system. Moreover, the yaw rate, the roll rate and the roll angle of the proposed controller are closer to the defined objectives.

In the second part of the simulations, some disturbances are applied to the mass, the yaw moment of inertia, the longitudinal velocity and the road conditions. In addition, a wind in the lateral direction with a force equal to 85.5 N at $t = 5$ sec. is applied to the vehicle.

In view of the goals of 4WS control system, simulation results, shown in Figs. 5-9, exhibit better performance for the proposed controller as compared to other advanced controllers (i.e. the SMC and the fuzzy SMC) against changes in the vehicle parameters and lateral wind. First, the mass and the yaw moment of inertia of the vehicle are changed according to the following equations [29]:

$$m = (1+p)m, \quad \hat{I}_{zz} = I_{zz} + p \cdot m \cdot L_r^2,$$

where $p = 0.05$.

Figs. 5-7 depict the results for the change in the mass, the yaw moment of inertia and the longitudinal speed of the vehicle ($\Delta V_X = 60$ Km/h), respectively. According to these figures, the body side-slip angle is less for the proposed hybrid SMC-SFC controller as compared to the SMC and fuzzy SMC controllers. In addition, the yaw rate of the proposed controller has faster transient response and less steady-state error. Moreover, the role angle of the proposed hybrid controller is smoother than the other two controllers.

Fig. 8 shows the simulation results for changes in the road conditions, in which the vehicle moves from a dry road (slip coefficient equal to 0.05) to a road where the right wheels are running on a wet surface (slip coefficient equal to 0.12) and the left wheels are on a snowy surface (slip coefficient equal to 0.2). These changes take place at $t = 5$ sec. As it can be observed from this figure, the hybrid SMC-SFC has the least variations in the yaw rate with smallest transient time and less steady-state error. Moreover, the fuzzy

SMC has less body side-slip angle than the SMC, but more than the hybrid SMC-SFC. In addition, the SMC exhibits more variations in the movement directions of the vehicle, especially when the road conditions change. Nevertheless, the roll angle of the fuzzy SMC is smoother than the proposed controller. However, the proposed SMC-SFC shows fewer variations in the roll rate, before applying the new road conditions. On the other hand, the fuzzy SMC yields fewer variations in the roll rate after the new road conditions are applied.

Fig. 9 depicts how different controllers perform against a cross wind disturbance applied to 0.5 m above the centre of gravity of the vehicle, in the lateral direction, with a force equal to 85.5 N at $t=5$ sec. As the diagrams in this figure show, the proposed hybrid SMC-SFC is more robust against this disturbance, as compared to other two controllers. In this case, the proposed controller outperforms the fuzzy SMC and the SMC in the yaw rate, the body side-slip angle, the roll angle and the roll rate. Moreover, the transient responses and the steady-state errors of the hybrid SFC-SMC are much better than the SMC and the fuzzy SMC, before and after applying the disturbance.

Finally, Fig. 10 shows how the transition takes place form the SMC to the SFC, and vice versa, in the proposed controller, for the case of Fig. 4. As this figure shows, the contribution of the SMC is higher when the state variables are far from the desired values. On the other hand, the SFC is the main controller when the state variables are closed to the desired values. Moreover, the transition between these controllers is continuous and smooth due to the employment of fuzzy logic in the proposed method.

6. Conclusion

In this paper, a hybrid control method for better handling of the four-wheel-steering system is proposed. The proposed method combined a sliding-mode controller and a state-feedback controller using the fuzzy logic. The designed fuzzy system takes advantage of either a sliding-mode controller or a state-feedback controller in the consequent part of the fuzzy IF-THEN rules. Therefore, the advantages of both controllers are brought together in one control method. Moreover, the stability of the proposed control method is guaranteed using the Lyapunov stability theory. Simulation results are compared with the sliding-mode controller and the fuzzy sliding-mode controller. The results show good performances of the proposed method which are faster yaw rate, less body side-slip angle, less roll angle, smoother roll rate and better stability when disturbances are applied to the vehicle and to the environment conditions.

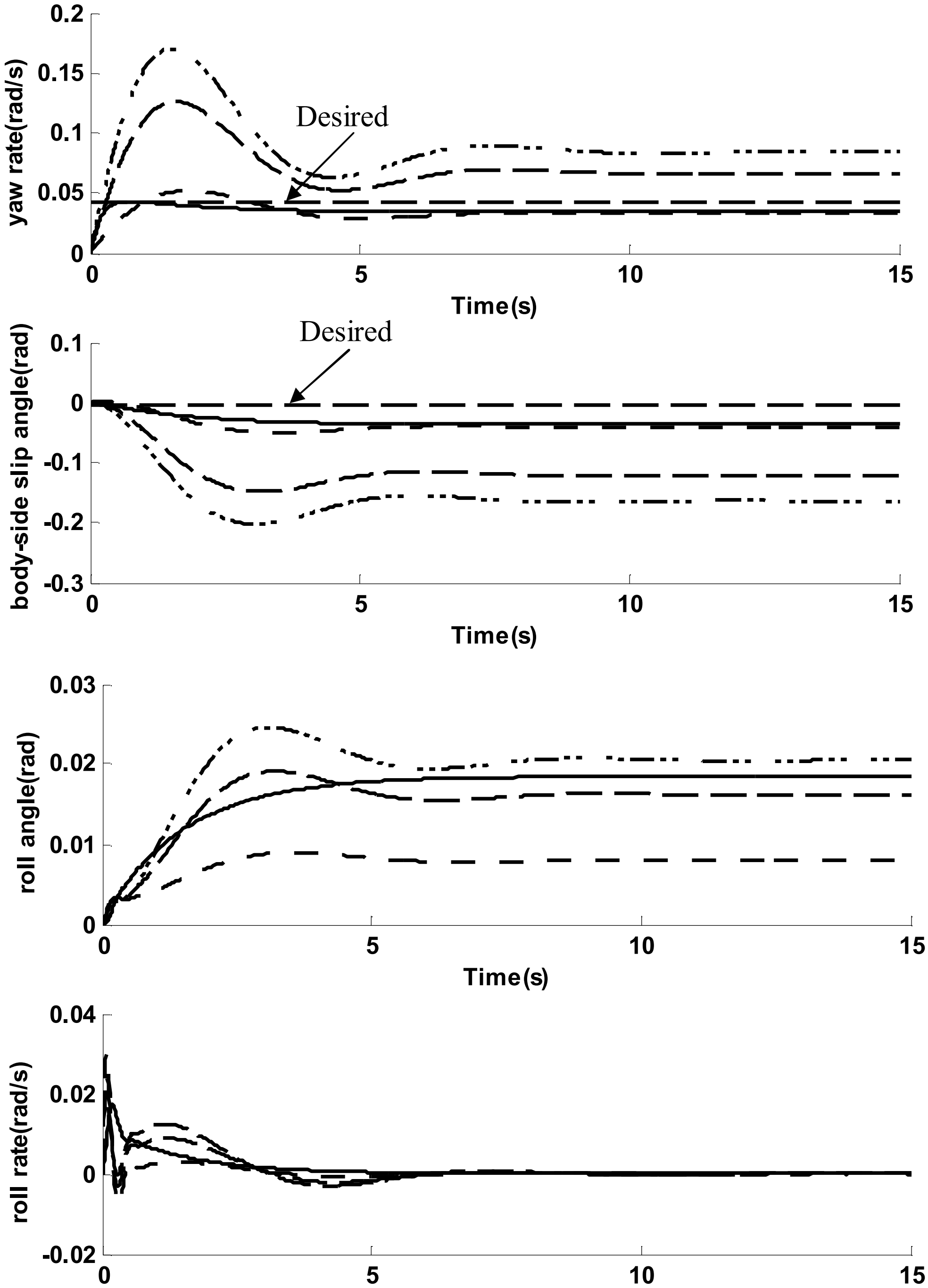

Fig. 4: Performance of the 4WS vehicle with the hybrid controller (—), fuzzy SMC (···), SMC (– –) and the 2WS vehicle (–·).

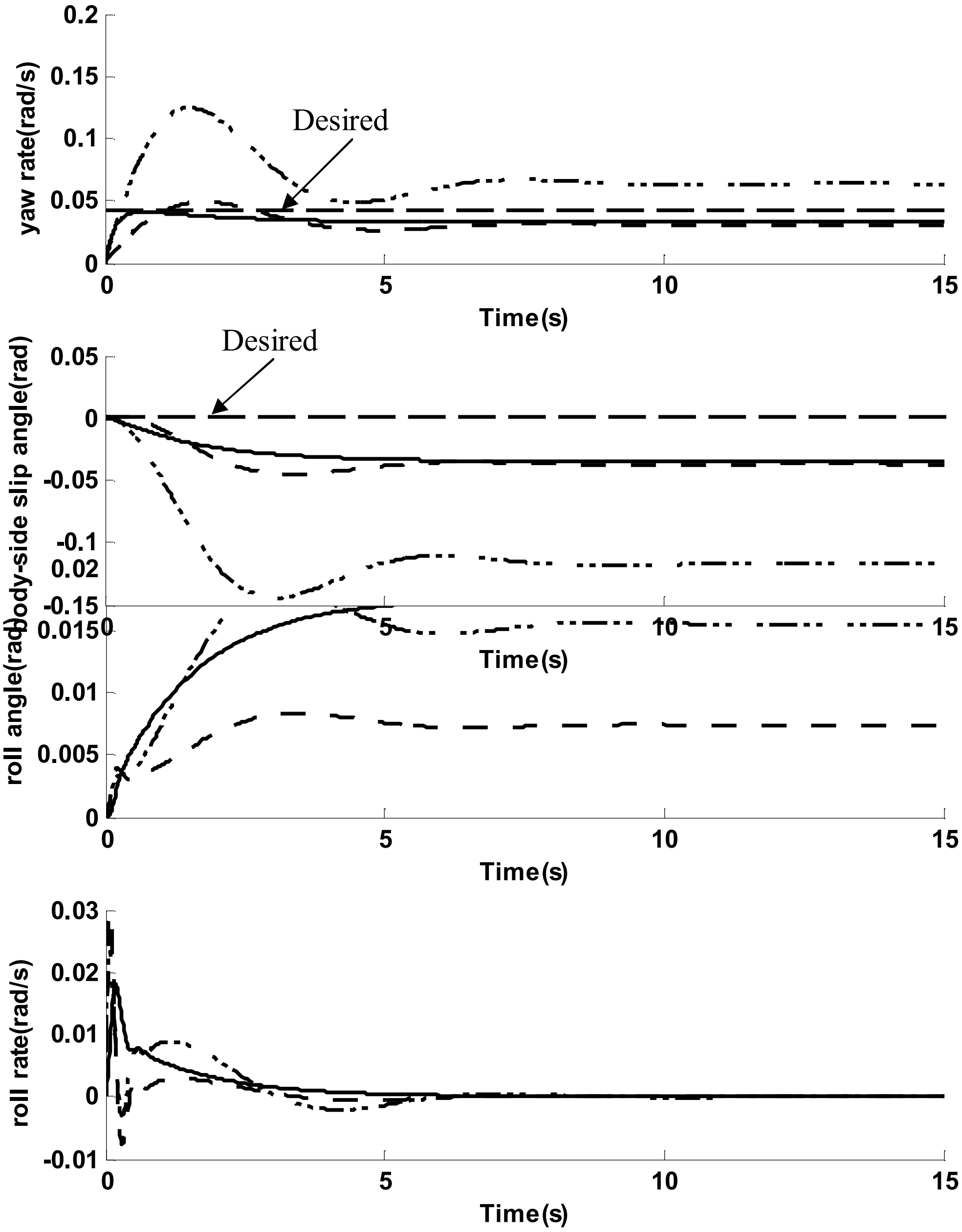

Fig. 5: Performance of the 4WS vehicle with the hybrid controller (—), fuzzy SMC (···) and SMC (−·), when the mass of vehicle changes.

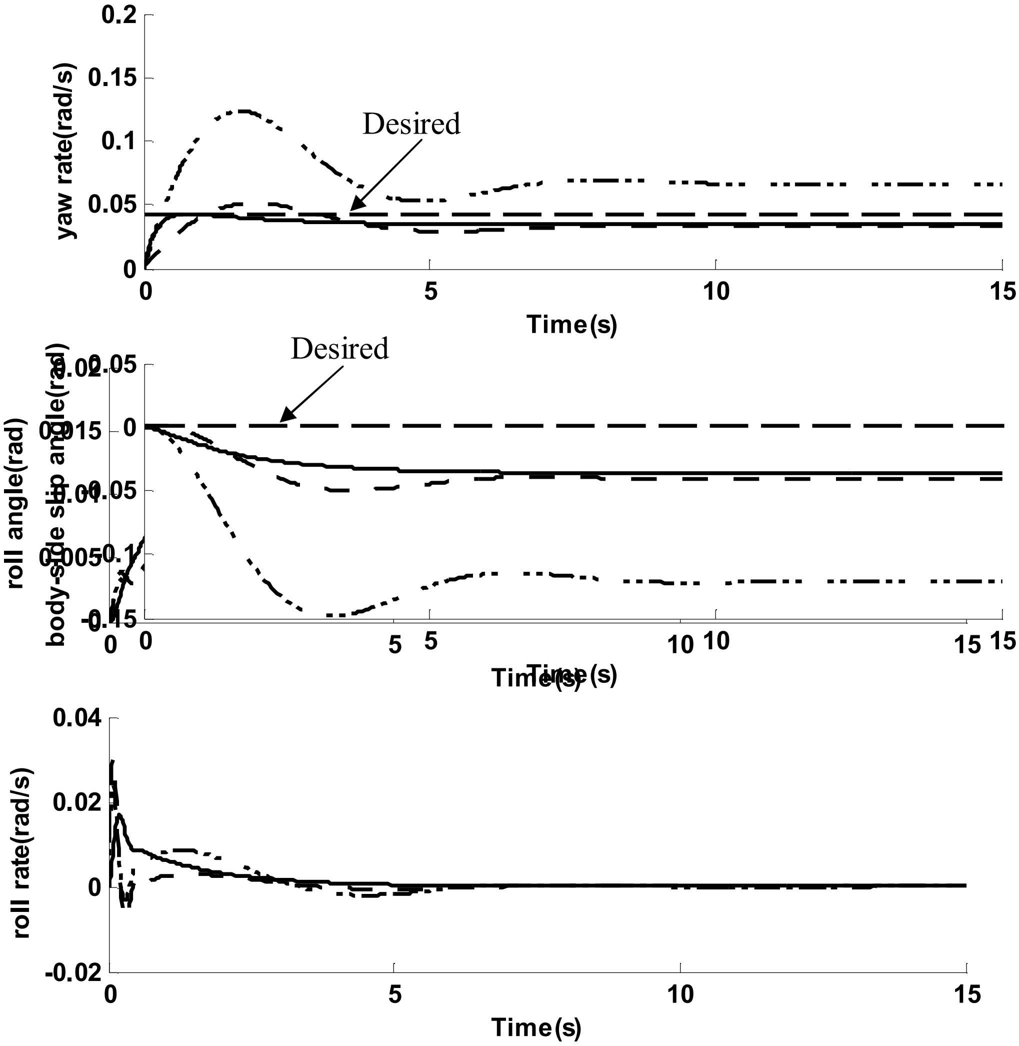

Fig. 6: Performance of the 4WS vehicle with the hybrid controller (—), fuzzy SMC (···) and SMC (−·), when the yaw moment of inertia changes.

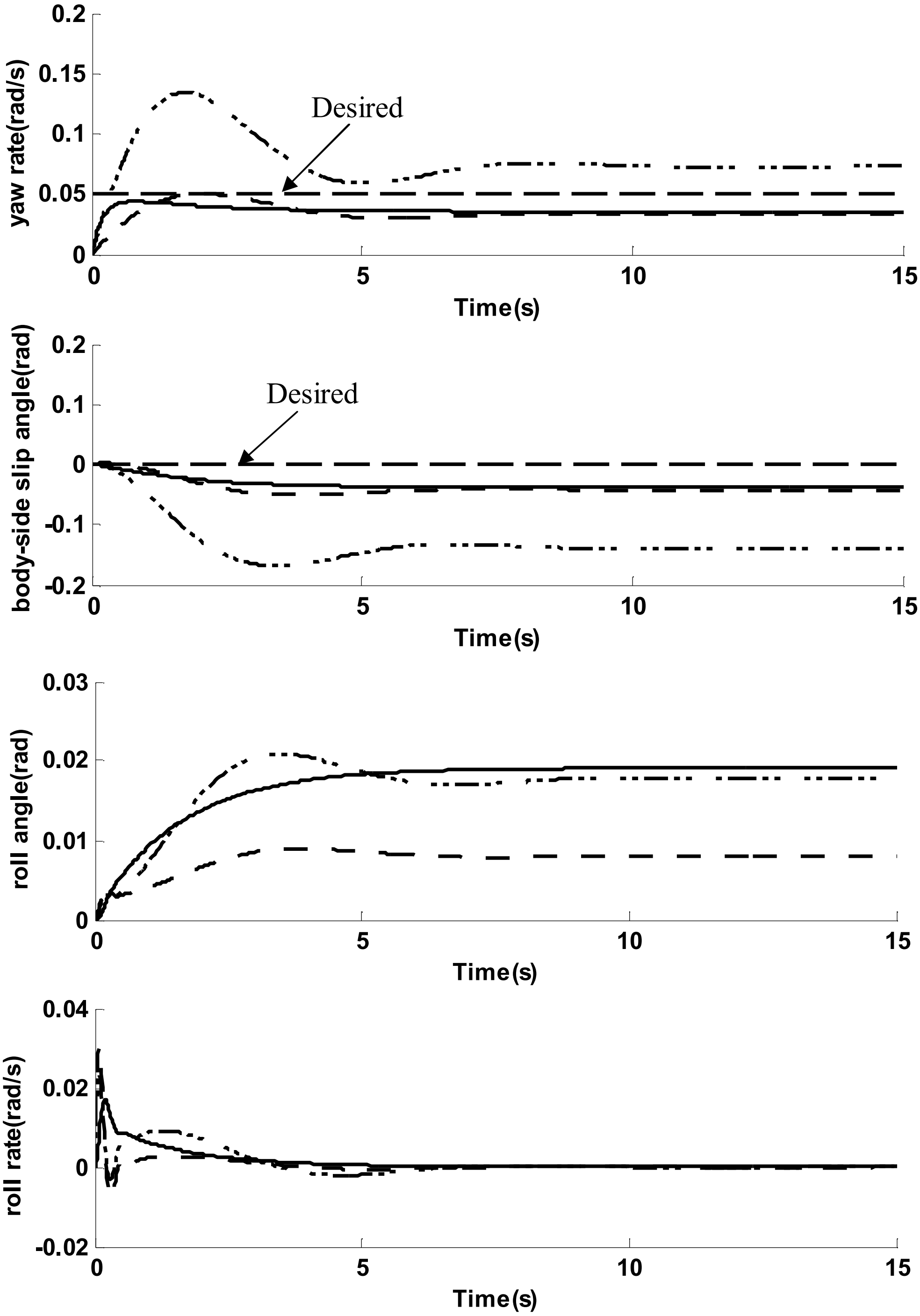

Fig. 7: Performance of the 4WS vehicle with the hybrid controller (—), fuzzy SMC (···) and SMC (−·), when the longitudinal speed of vehicle changes ($\Delta V_X = 60$ Km/h).

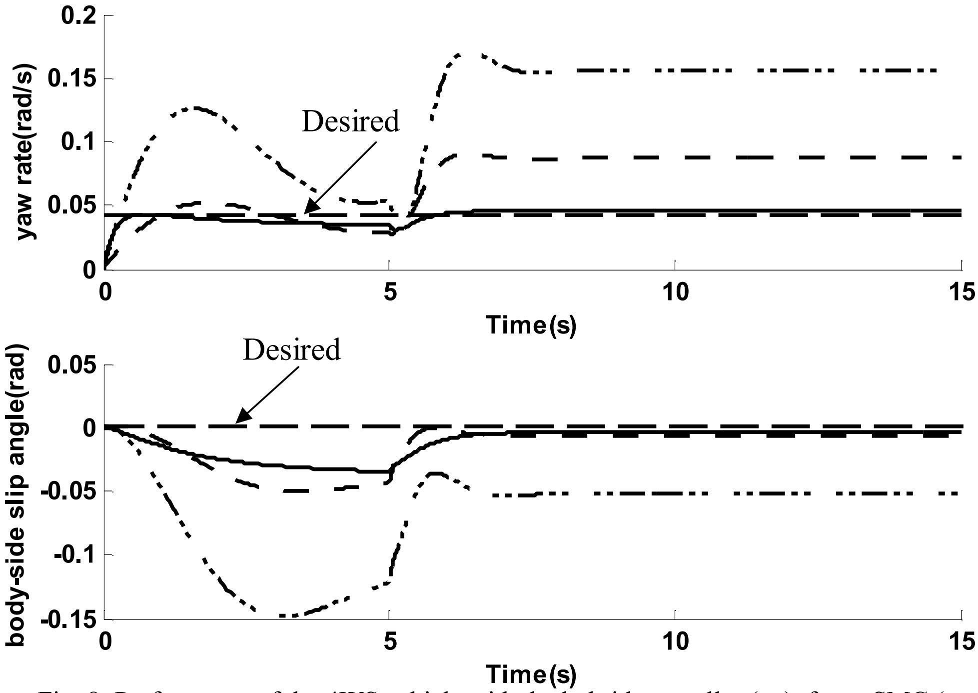

Fig. 8: Performance of the 4WS vehicle with the hybrid controller (—), fuzzy SMC (···) and SMC (−·), when the road conditions change to $S_R = 0.2$ and $S_L = 0.12$, respectively.

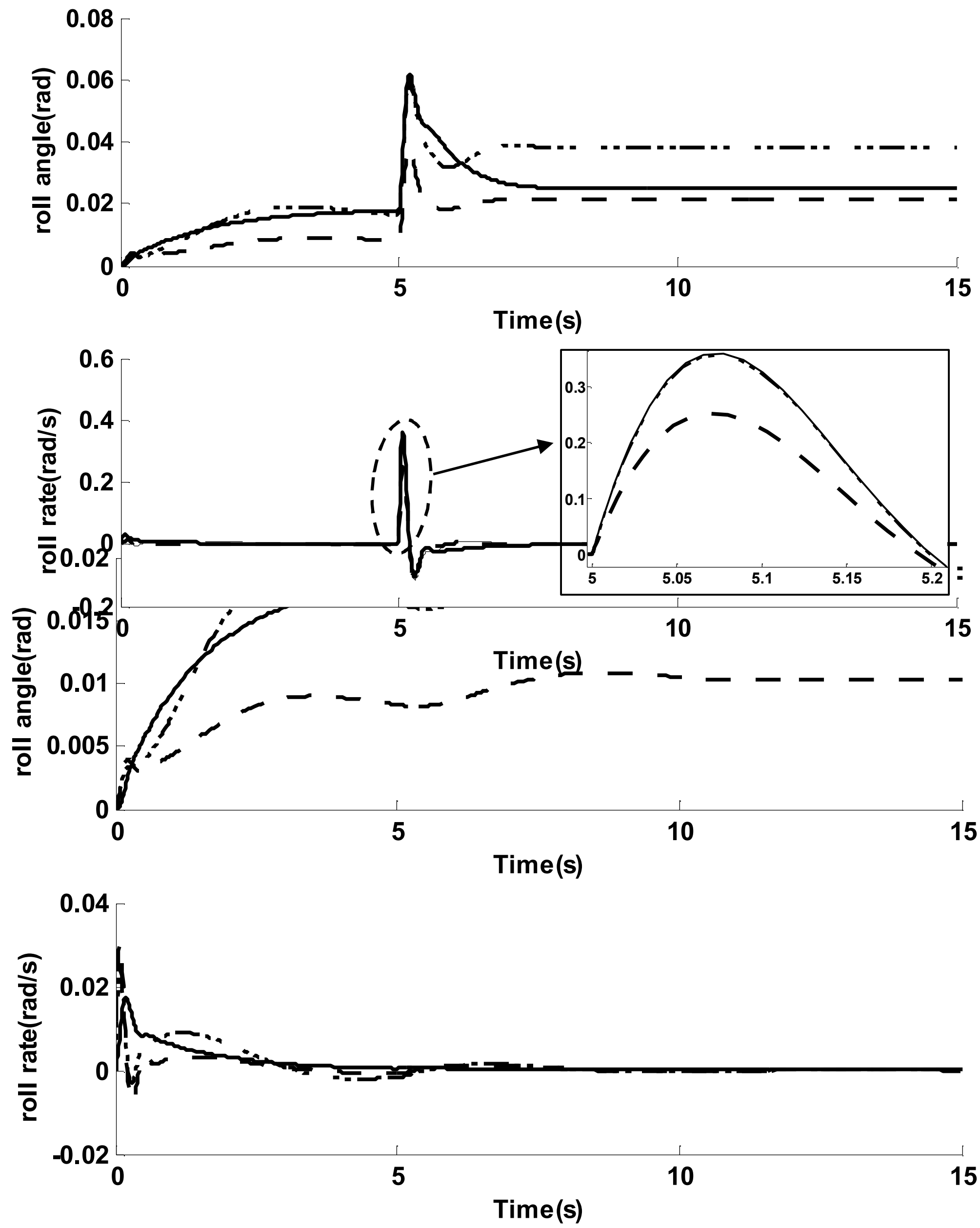

Fig. 9: Performance of the 4WS vehicle with the hybrid controller (—),
Fuzzy SMC ($\cdots$) and SMC (— ·), when the vehicle encounters disturbances from the environment
(Lateral wind with $d = 0.25$ m and $F = 85.5$ N).

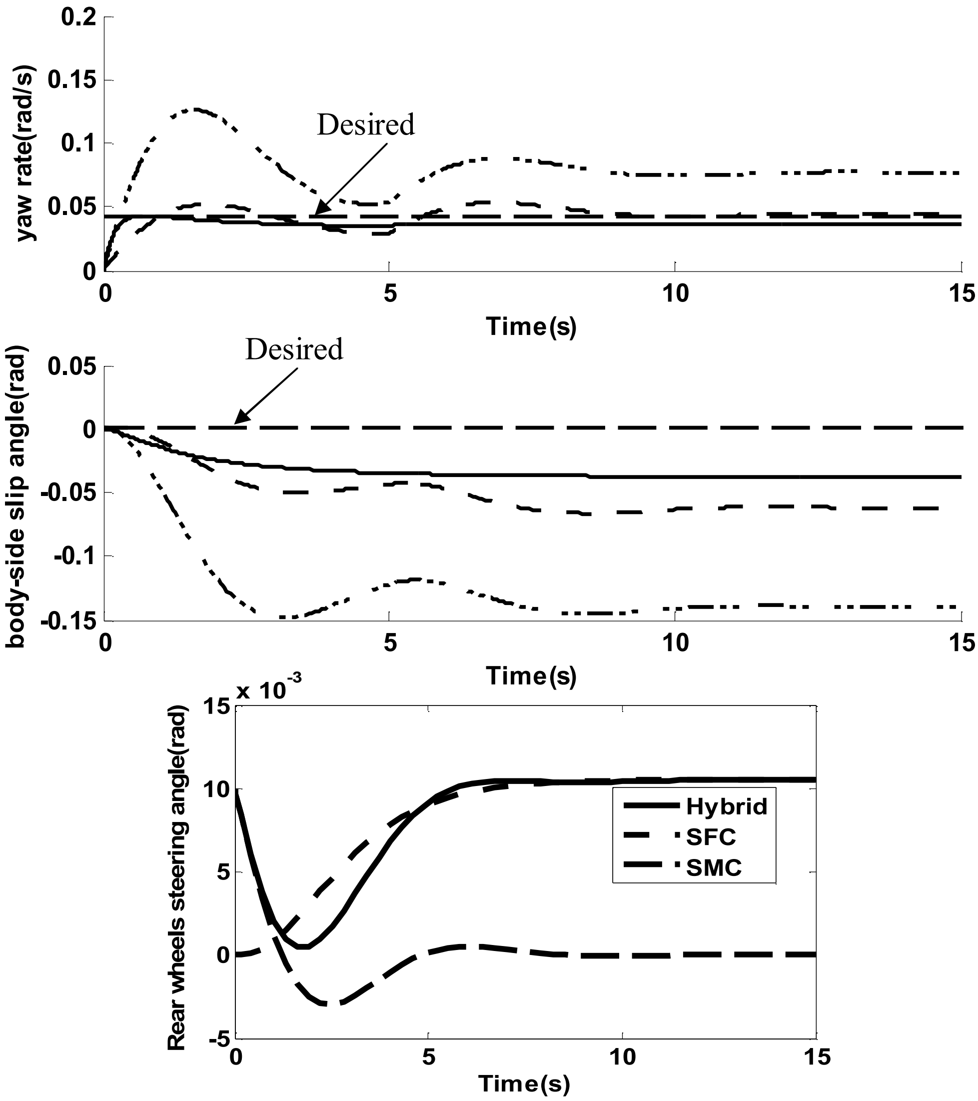

Fig 10: Contribution of the SFC and the SMC to the control law for the case of Fig. 4.

Table 1: vehicle parameters

Parameters	Parameters
spring mass m_s = 1167.5 Kg	total mass m = 1298.84 Kg
distance from c.g.[1] of the front axis L_f = 1 m	front spring mass m_{uf} = 65.67 Kg
distance from c.g. of the rear axis L_r = 1.45 m	rear spring mass m_{ur} = 65.67 Kg
height of sprung mass of c.g. h = 0.4572 m	yaw moment of inertia I_{zz} = 1627 Kgm^2
height of front effective roll center h_f = 0.1219 m	roll moment of inertia I_{xx} = 489.9 Kgm^2
height of rear effective roll center h_r = 0.0887 m	roll-yaw cross inertia I_{xz} = 0 Kgm^2
height of the front unsprung mass at c.g. h_{uf} = 0.3048 m	roll stiffness produced by the front springs $L_{\varphi f}$ = 37300 N.m/rad
height of the rear unsprung mass at c.g. h_{ur} = 0.3048 m	roll stiffness produced by the rear springs $L_{\varphi r}$ = 30500 N.m/rad
height of c.g. of center axis h_o = 0.10835 m	roll damping produced by the front shock absorbers $L_{\dot{\varphi} f}$ = 1756 N.m.s/rad
longitudinal velocity V_x = 33.33 m/s	roll damping produced by the rear shock absorbers $L_{\dot{\varphi} r}$ = 1756 N.m.s/rad

[1] center of gravity

APPENDIX A. Tyre Model

The tyre model used in this paper has been effective in replicating experimental observations of nonlinear behavior in tyres. The transition from slipping to complete sliding shows the force saturation behavior observed in tyre tests [21], [30]. In tyre modeling, the interaction between the longitudinal and lateral forces is the most important factor. In this model, these forces are calculated as follows.

First, the lateral stiffness coefficient k_s, the longitudinal stiffness coefficient k_c, the maximum coefficient of friction μ_o and the tyre constant patch length a_p are calculated as

$$k_s = \frac{2\left[A_0 + A_1 F_z - {A_1}/{A_2}\, F_z^2\right]}{a_{p_0}^2} \quad , \quad a_p = a_{p_o}\left[1 - k_a\left({F_x}/{F_z}\right)\right]$$

$$k_c = \frac{2F_z\left({cs}/{F_z}\right)}{a_{p_0}^2} \quad , \quad \mu_o = 1.176\mu_{\text{nom}}\left(B_3 + B_1 F_z + B_4 F_z^2\right),$$

where $a_{p_o} = \dfrac{0.0768\sqrt{F_z F_{zT}}}{T_w\,(T_p + 5)}$ is the initial tyre patch length, F_z is the total normal load, F_{zT} is the tyre design load at the operating pressure, T_w is the tread width, T_p is the tyre pressure, k_a is the proportional effect of F_x on patch length, cs / F_z is the coefficient obtained from the Calspan test, A_i $(i = 0, 1, 2)$ are the Calspan cornering stiffness coefficients, B_i $(i = 1, 3, 4)$ are the Calspan peak lateral friction coefficients, and μ_{nom} is the nominal coefficient of friction.

Second, the composite slip function σ and the tyre saturation function $f(\sigma)$ can be determined as

$$\sigma = \frac{\pi a_p^2}{8\mu_o F_z}\left[k_s^2 \tan^2\alpha + k_c^2\left(\frac{s}{1-s}\right)^2\right], \quad f(\sigma) = \frac{c_1\sigma^3 + c_2\sigma^2 + {4}/{\pi}\,\sigma}{c_1\sigma^3 + c_3\sigma^2 + c_4\sigma + 1},$$

where c_i $\left(i=1, 2, 3, 4\right)$ are the coefficients for the saturation function, s is the slip coefficient and α is the tyre slip angle. The other parameters are the same as defined before.
The transition longitudinal stiffness coefficient k_c' and the transition coefficient of friction μ are calculated as

$$k_c' = k_c + \left(k_s - k_c\right)\sqrt{\sin^2\alpha + s^2\cos^2\alpha}, \quad \mu = \mu_o\sqrt{1-k_\mu\,(\sin^2\alpha + s^2\cos^2\alpha)}\,,$$

where $k_\mu = {V_{wl}^{1/4}}\big/{11}$ is the transition constant, and V_{wl} is the velocity of tyre.
Finally, the tyre lateral and longitudinal forces are calculated as

$$F_y = \mu F_z \frac{\left[f\left(\sigma\right)k_s \tan\alpha\right]}{\left[k_s^2\tan^2\alpha + k_c'^2 s^2\right]^{1/2}}, \quad F_x = \mu \;\; F_z \frac{\left[-f\left(\sigma\right)k_c' \tan\alpha\right]}{\left[k_s^2\tan^2\alpha + k_c'^2 s^2\right]^{1/2}}.$$

The slip angles are described as

$$\alpha_{fr} = \delta_f - \tan^{-1}\left(\frac{V_y + L_f r}{V_x - \frac{d_f}{2}}\right) + \frac{\partial\alpha_f}{\partial\varphi}\varphi \quad , \quad \alpha_{fl} = \delta_f - \tan^{-1}\left(\frac{V_y + L_f r}{V_x + \frac{d_f}{2}}\right) + \frac{\partial\alpha_f}{\partial\varphi}\varphi$$

$$\alpha_{rr} = \delta_r - \tan^{-1}\left(\frac{V_y - L_r r}{V_x - \frac{d_r}{2}}\right) + \frac{\partial\alpha_r}{\partial\varphi}\varphi \quad , \quad \alpha_{rl} = \delta_r - \tan^{-1}\left(\frac{V_y - L_r r}{V_x + \frac{d_r}{2}}\right) + \frac{\partial\alpha_r}{\partial\varphi}\varphi$$

where d_f and d_r are the front and the rear track width, respectively. The normal loads on tyres have the following relations [21]:

$$N_{fl} + N_{rl} + N_{fr} + N_{rr} = Mg \quad , \quad L_f\,(N_{fl} + N_{fr}) - L_r\,(N_{rl} + N_{rr}) = 0\,,$$

$$(N_{fr} - N_{fl})\frac{d_f}{2} = L_{\varphi f}\,\varphi + L_{\dot{\varphi} f}\,\dot{\varphi} \quad , \quad (N_{rr} - N_{rl})\frac{d_r}{2} = L_{\varphi r}\,\varphi + L_{\dot{\varphi} r}\,\dot{\varphi}\,.$$

Rearranging these equations gives

$$N_{fr} = \frac{MgL_r}{2(L_f + L_r)} + \frac{L_{\varphi f}\,\varphi + L_{\dot{\varphi} f}\,\dot{\varphi}}{d_f} \quad , \quad N_{fl} = \frac{MgL_r}{2(L_f + L_r)} - \frac{L_{\varphi f}\,\varphi + L_{\dot{\varphi} f}\,\dot{\varphi}}{d_f}$$

$$N_{rr} = \frac{MgL_f}{2(L_f + L_r)} + \frac{L_{\varphi r}\varphi + L_{\dot{\varphi} r}\dot{\varphi}}{d_r} \quad , \quad N_{rl} = \frac{MgL_f}{2(L_f + L_r)} - \frac{L_{\varphi r}\varphi + L_{\dot{\varphi} r}\dot{\varphi}}{d_r}$$

Tables 2 and 3 show typical values for the coefficients and the saturation function $f\left(\sigma\right)$ of different tyres, respectively. Notice that, μ_{nom} has a value of 0.85 for normal road conditions; it is equal to 0.3 for wet conditions, and 0.1 for icy road conditions.

Table 2: Parameters for three different tyres

Parameter	Standard Cross Section Radial (RWD)	Biasply (RWD)	Wide Section Low-profile Radial (FWD)
Tyre Designation	155R13	P155.80D13	P185.70R13
T_w	6	6	7.3
T_p	24	24	24
F_{zT}	810	900	980
A_0	914.02	1817	1068
A_1	12.9	7.48	11.3
A_2	2028.24	24.55	2442.73
k_a	0.05	0.2	0.05
B_1	3.36e-4	2.57e-4	1.69e-4
B_3	1.19	1.19	1.19
B_4	4.98e-8	2.64e-8	1.69e-8
cs / F_z	18.7	15.22	17.91
μ_{nom}	0.85	0.85	0.85

Table 3: coefficients of the saturation function

Tyre Type	c_1	c_2	c_3	c_4
Biasply	0.535	1.05	1.15	0.8
Radial	1	0.34	0.57	0.32

APPENDIX B. Fuzzy-Sliding System

In designing a fuzzy-sliding controller, using sup-min compositional rule of inference, singleton fuzzifier, and center of gravity defuzzifier, the crisp output u_c can be found as [31]

$$u_c = \frac{\int u_f \cdot \mu(u_f) du_f}{\int \mu(u_f) du_f},$$

where μ_F is the deduced membership function of the consequences of all rules. The fuzzy IF-THEN rules for the fuzzy-sliding controller are defined as

Rule 1: IF s is NB THEN u_f is Bigger

Rule 2: IF s is NM THEN u_f is Big

Rule 3: IF s is Z THEN u_f is Medium

Rule 4: IF s is PM THEN u_f is Small

Rule 5: IF s is PB THEN u_f is Smaller

where NB, NM, Z, PM, and PB are labels for fuzzy sets and stand for negative big, negative medium, zero, positive medium, and positive big, respectively, k_f is the span of fuzzy sets, and s is the sliding surface. The corresponding membership functions for the fuzzy sets are shown in Figs. B1 and B2, respectively.

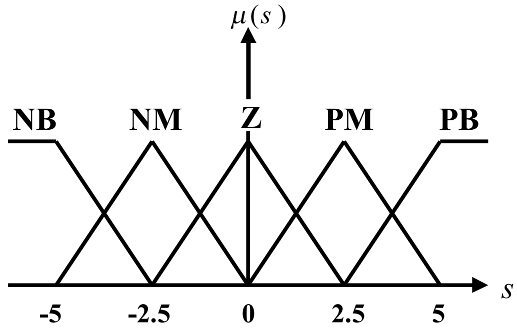

Fig. B1: Membership functions for the input variable

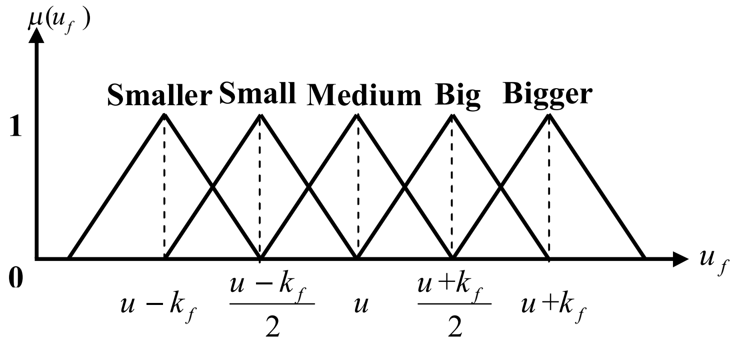

Fig. B2: Membership functions for the output variable (i.e. the sliding surface)

References

[1] Wang, J.W., 1993, *Theory of Ground Vehicles*, 2nd Ed., (New York: John Wiley & Sons).

[2] Allen, R. W., Rosenthal, T. J., and Wu, H. T. S., 1987, Steady-state and transient analysis of ground vehicle handling. *SAE Paper no. 901 746.*

[3] Furukawa, Y., Yuhara, N., Sano, S., Fakeda, H., and Matsushita Y., 1989, A review of four-wheel steering studies from the viewpoint of vehicle dynamics and control. *Vehicle System Dynamics*, 151--186.

[4] Irie, N. and Kuroki, J., 1990, 4WS technology and the prospects for improvement of vehicle dynamics. *SAE Paper no. 901 167.*

[5] Koresawa M. and Shimosaka, H., 1994, Study on a four wheel steering vehicle driven at an objective side-slip angle. *JSAE Review*, **15**(1), 45--51.

[6] Itoh, H., Oida, A., and Yamazaki, M., 1995, Measurement of forces acting on 4WD-4WS tractor tyres during steady-state circular turning in a rice field. *Journal of Terramechanics*, **32**(5), 263--283.

[7] Gianone, L., Palkovics, L., and Bokor, J., 1995, Design of an active 4ws system with physical uncertainties. *Control Engineering Practice*, **3**(8), 1075--1083.

[8] Horiuchi, S., Okada, K., and Nohtomi, S., 1999, Improvement of vehicle handling by nonlinear integrated control of four wheel steering and four wheel torque. *JSAE Review*, **20**(4), 459--464.

[9] You S. S. and Chai, Y. H., 1999, Multi-objective control synthesis: an application to 4WS passenger vehicles. *Mechateronics*, **9**(4), 363--390.

[10] Itoh, H., Oida, A., and Yamazaki, M., 1999, Numerical simulation of a 4WD–4WS tractor turning in a rice field. *Journal of Terramechanics*, **36**(2), 91--115.

[11] Huh, K., Seo, C., Kim, J., and Hong, D., 1999, Active steering control based on the estimated tyre forces. *Proceedings of the American Control Conference*, 729--733.

[12] Haiyan H., and Zhiqiang, W., 2000, Stability and Hoff bifurcation of four-wheel-steering vehicles involving driver's delay. *Nonlinear Dynamics*, **22**(4), 361--374.

[13] Wang, B., Abe, M., and Kano, Y., 2002, Influence of driver's reaction time and gain on driver–vehicle system performance with rear wheel steering control systems: part of a study on vehicle control suitable for the aged driver. *JSAE Review*, **23**(1), 75--82.

[14] Akita, T. and Satoh, K., 2003, Development of 4WS control algorithms for an SUV. *JSAE Review*, **24**(4), 441--448.

[15] Dai, L. and Han, Q., 2004, Stability and Hoff bifurcation of a nonlinear model for a four-wheel-steering vehicle system. *Communications in Nonlinear Science and Numerical Simulation*, **9**(3), 331-341.

[16] Raksincharoensak, P., Mouri, H., and Nagai, M., 2004, Evaluation of four-wheel-steering system from the view point of lane keeping control. *International Journal of Automotive Technology*, **5**(2), 69-76.

[17] Farrokhi M. and Alfi, A., 2002, Adaptive fuzzy controller for handling improvement of four-wheel-steering vehicle. *Proceedings of 15th IFAC Triennial World Congress*, Barcelona.

[18] Wang, L. X., 1997, *A Course in Fuzzy System and Control*, (New Jercy: Prentice Hall).
[19] Tanaka, T. and Sugeno, M., 1993, Stability analysis and design of fuzzy control systems. *Fuzzy Sets and Systems* **57**(2), 125-140.
[20] Wang, H. O., Tanaka K., and Griffin, F., 1996, An approach to fuzzy control of nonlinear systems: stability and design issues. *International Journal of System and Science*, **27**(2), 14-23.
[21] Ohnuma, A. and Metz, L. D., 1989, Controllability and stability aspect of actively controlled 4WS vehicles. *SAE Paper no. 891 977*, 1481-1494.
[22] Gillespie, T. D., 1992, *Fundamentals of vehicle dynamics*, (SAE International).
[23] Song, J. G. and Yoon, Y. S., 1998, Feedback control of four-wheel steering using time delay control. *International Journal of Vehicle Design*, **19**(3), 282-298.
[24] Slotine, J. J. and Li, W., 1991, *Applied Nonlinear Control*, (New Jercy: Prentice Hall).
[25] Teixeira, M. C. M., Zak, S. H., and Will, A. B., 1997, Four wheel steering control system design using fuzzy models. *Proceedings of the Conference Control Applications,* 73-78.
[26] Kirk, D. E., *An Introduction to Optimal Control Theory*, 1970, (New Jercy: Prentice-Hall).
[27] Wong, L. K., Leung, H. F., and Tam, K. S. P., 1998, Lyapunov-function-based design of fuzzy logic controllers and its application on combining controllers. *IEEE Transactions on Industrial Electronics*, **45**(3), 502-509.
[28] Wong, L. K., Leung H. F., and Tam, K. S. P., 2001, A fuzzy sliding controller for nonlinear systems. *IEEE Transactions on Industrial Electronics*, **48**(1), 32-37.
[29] Yeh, E. C. and Wu, R. H, 1989, Open-loop design for decoupling control of a four-wheel-steering vehicle. *International Journal of Vehicle Design*, **10**(5), 531-552.
[30] Nalecz, A. G., and Bindemann A. C., 1980, Handling properties of four wheel steering vehicles. *SAE Paper no. 890 080*, 63-80.
[31] Lo J. C. and Kuo, Y. H., 1998, Decoupled fuzzy sliding-mode control. *IEEE Transactions on Fuzzy Systems*, **6**(3), 426-435.